

# Mâadid Clay In The M'sila Region, Algeria: Evaluation And Characterization

Deghfel Nadir<sup>1</sup>, Benyahia Azzedine<sup>2</sup>, Hamrouni Achraf<sup>3</sup>, Rahmouni Zine El Abidine<sup>4</sup>,  
Nouioua Khaoula<sup>1</sup>, Belaâda Hanane<sup>1</sup>, Dahmoune Karima<sup>1</sup>

<sup>1</sup> University Mohamed Boudiaf M'sila, Algeria.

<sup>2</sup> Laboratory of City, Environment, Society and Sustainable Development, University of Med Boudiaf, M'sila, Algeria.

<sup>3</sup> University Badji Mokhtar Annaba, Algeria.

<sup>4</sup> Geo materials Development Laboratory, University of Med Boudiaf, M'sila, Algeria.

---

## Abstract

This work aims to valorize local materials, such as the clay of southern Algeria, widely used to prepare bricks as rural construction materials. We characterized and identified three types of natural clays from the region of Mâadid province of M'sila. The results show that the yellow clay is a mixture of quartz illite in a very important proportion since the percentage of illite was 47%. While in the green clay, we noted that the predominant constituents are: calcite, quartz, illite, and kaolinite, and the highest percentage is illite was 27.93%. The analytical results show that the red clay is a calcite, quartz, and illite mixture. Several techniques were used: XRD, XRF, FTIR.

**Keywords:** red clay, rural construction, swelling coefficient, colloidal, plasticity

---

## I. Introduction

The world faces great challenges due to an increasing quantity of emitted gases, causing global warming. There are many sources of greenhouse gas emissions. The most important is the construction industry, which consumes a large amount of energy and emits significant greenhouse gases [1-4]. With population growth and the need for building materials, interest in suitable materials such as clay has piqued the research community's interest. Clay, for example, has been used in construction as an alternative to cement and rubble, to reduce these emissions that contribute to environmental pollution [5-8], clay-based building materials can be used, especially in rural construction, because of its advantages, including low environmental impact, thermal insulation, limited shrinkage, high strength and low-cost [9-14]. Some studies have used the characterization of different types of clay used as compressed earth blocks and reinforced with plant fibers to prepare composite materials for rural construction [15]. Koadri et al. [15] studied the effect of alkali treatment on the mechanical

behavior of a red clay-composite material reinforced with palm fibers. The authors found from the spectral analysis of the diffractogram that the red clay is heterogeneous, with high proportions of quartz compound ( $\text{SiO}_2$ ) calcite  $\text{CaCO}_3$ . Mouissa et al. [16] examined the effect of chemical treatment of sawdust on the mechanical and thermal properties of a clay-based composite from the Bou-Saâda region, intended for use as a rural construction material. The chemical analysis of clay revealed that silica and alumina are the main oxides of the sample studied. Their percentages are respectively 35.21% and 13.62%. Thus, the studied clay is an aluminosilicate rich in calcite ( $\text{CaCO}_3$ ).

Phung et al. [17] investigated the mechanical strength and drying capacity of mud made from three different soils currently used for conventional earth construction. Two earth-fiber formulations were developed using straw as fiber. The results show that the compressive strength increases as the moisture content decreases. This research aims to develop environmentally friendly, thermally insulating, and low-cost materials used in rural construction. Clay is a very abundant material in Algeria (Figure1).



**Fig.1** Mountain with Mâadid clay.

Source: Authors (January 2022)

## II. Materials and methods

For this work, we collected a sample of red clay from the region of Al-Maâdid, located 35 km north of M'sila, and two samples of yellow clay and green clay from the region of Ouled Tebbene, wilaya of Setif, northeast Algeria. The samples collected underwent the following unit operations:

- the rocks of the sample were crushed in pieces using a mortar;
- the clay sample pieces were ground in a mill;
- the sample powder was sieved (50 $\mu\text{m}$  sieve);
- the samples were dried in the oven for 24 h ( $T=105\text{ }^\circ\text{C}$ ).

### Determination of pH

A 10% solution of each clay m/v was prepared with distilled water. The mixture was left to rest for 4h at 25° C to allow the ions to pass into the solution. The clay solution obtained was homogenized by a magnetic stirrer. The reading was done directly on a HANNA pH meter (pH 211 made in Italy) [18-21].

### Moisture content

Moisture content measurement determines the moisture mass removed by drying a wet material to a constant mass at a temperature of  $105 \pm 5$  °C for 24 h. The mass of the material after steaming is considered to be the mass of the solid particles ( $m_s$ ). The determination of the moisture content is calculated from the ratio of the mass of moisture ( $m_{\text{moisture}}$ ) to the mass of solid particles ( $m_s$ ). This gives the moisture content of the sample analyzed as proposed by Chossat(2005)[22]:

$$H(\%) = \frac{m_{\text{moisture}}}{m_s} \times 100 = \frac{m_t - m_s}{m_s} \times 100 \quad (1)$$

where,  $m_{\text{moisture}}$  is the moisture mass (g),  $m_s$  is the dry sample mass (g), and  $m_t$  is the wet sample mass (g).

### Density

The bulk density measurement of the studied sample was performed by determining the volume of a mass  $m$  of the sample using a pycnometer as follows:

$$\text{Density} = \frac{\text{Mass of the sample}}{\text{Volume of the sample}} \quad (2)$$

### Swelling index

By being suspended, the clay can fix a certain amount of water, which has the effect of moving away from each other, thus reflecting a swelling. A 100 ml graduated cylinder is filled with 50 ml of distilled water, and 0.5 g of clay is added. After 45 min, another 0.5 g of clay is added. After 2H, the swelling volume is noted. The swelling index is measured by the following formula (3) [23] :

$$\text{Swelling index (\%)} = \frac{\text{Swelling volume} \times 50}{50 - \text{humidity}} \times 100 \quad (3)$$

### Colloidalilty

This property is linked to the presence of negative charges on the surface of each clay grain. The covering of each clay grain translates the colloidal character by a double layer of water-soluble ions of opposite charges. Colloidalilty is measured by suspending a given quantity of clay adding 0.2g of MgO to allow deflocculation. After a 5 min agitation, the mixture is placed in a graduated test tube. After 24h, the volume  $V$  (ml) occupied by the supernatant is measured. The colloidalilty is measured with the following formula [24]:

$$C (\%) = 100 - V \quad (4)$$

X-ray diffraction analysis was used with an X'Pert High Score X-ray diffractometer (X'Pert Pro PW3209, Panalytical, made in France). Equatorial diffraction patterns ( $2\theta$ ) were recorded from  $10^\circ$  to  $40^\circ$  with Cu-K $\alpha$  radiation at 40 kV and 20 mA. The infrared spectra were studied using an FTIR apparatus (Shimadzu, FTIR-8300, made in Japan). The adsorption range was  $500 \text{ cm}^{-1}$  to  $4000 \text{ cm}^{-1}$ . The pellets were made by mixing 0.08 mg of clay with 0.01 mg of KBr. Furthermore, the mixture was subjected to a pressure of 80 Pa. The mineralogical test used X-ray fluorescence spectrometry. XRF Bruker AXS GmbH, Karlsruhe, Germany was used to analyze the mineralogical composition of clay. The elemental chemical analysis of the clay sample was performed using an XRF Spectrometer. This chemical analysis was carried out in the Lafarge Cimenterie M'sila plant laboratory.

## III. Results and discussion

### Mineralogical X-ray analysis

Table 1 summarizes the results of elemental chemical analysis obtained for the three clay samples. The diffractograms were obtained from the disoriented samples (placed directly in powder form in a conventional sample holder). Figures 2, 3, and 4 show the XRD pattern of three types of clays, respectively. Quartz at  $2\theta = 22^\circ$  and  $2\theta = 27^\circ$  was observed as a major impurity in the yellow and green clay samples (Figures 2 and 3). Calcite at  $2\theta = 29^\circ$  was present in the green and red clay samples. It was noted in a very small amount for the yellow clay sample. Reflections at  $2\theta = 31^\circ$  and  $2\theta = 42^\circ$  on the red clay prove the presence of dolomite (Figure 4). It can be observed that a peak at  $20^\circ$  appears on all three samples with different intensities. It can be attributed, presumably, to illite. Peaks at  $2\theta = 12^\circ$  and  $2\theta = 26^\circ$  on all three clay types indicate the presence of kaolinite. The clay fraction of the three types of clays include quartz, calcite, and dolomite. This result confirms that our clay samples are heterogeneous mixtures.

**Table. 1** Chemical analysis of clays.

Clay	Calcite (CaCO <sub>3</sub> )	Dolomite	Quartz (SiO <sub>2</sub> )	Pyrite- (FeS <sub>2</sub> )	Illite	Chlorite	Kaolinite	Albite	CO <sub>2</sub> XRD
Yellow	9.82	0	18.62	0	43.45	0	9.04	19.07	4.32
Green	18.93	3.86	27.04	0.37	27.93	3.1	14.28	4.47	10.17
Red	31.06	10.3	11.94	0.43	31.44	3.17	6.19	5.46	18.57

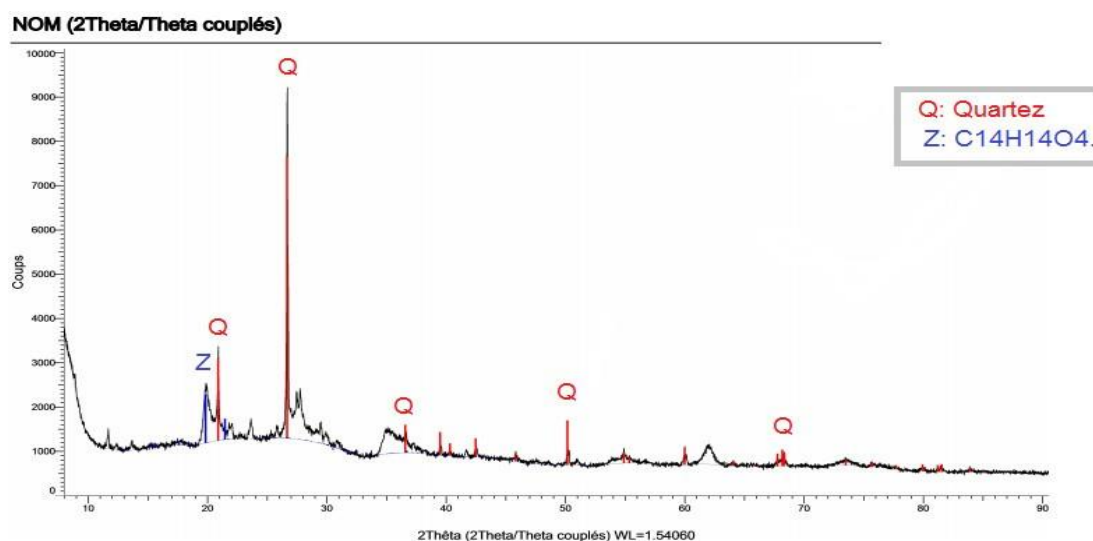


**Figure 2.** Histogram of the mineralogical DRX analyses of the yellow clay.

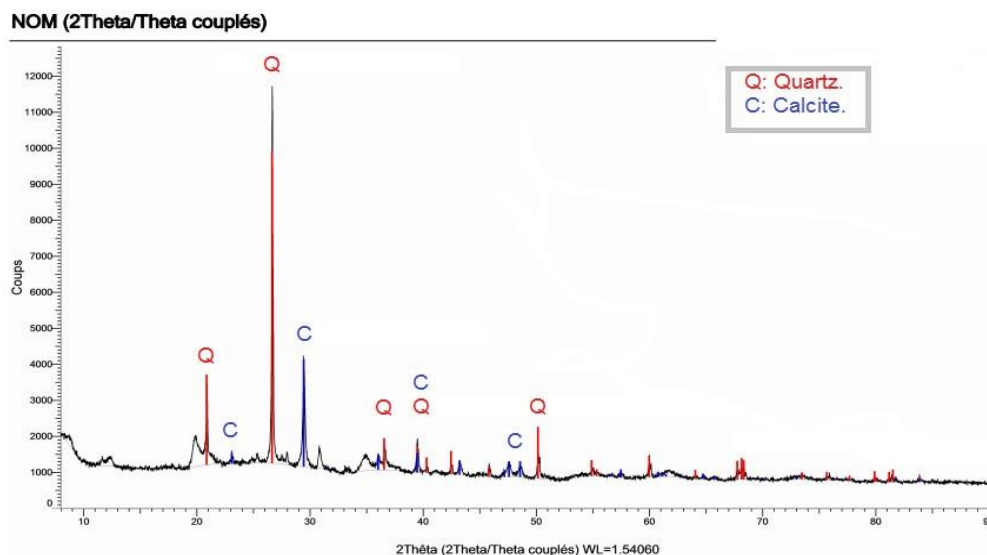


**Figure 3:** Histogram of the mineralogical DRX analyses of the green clay.

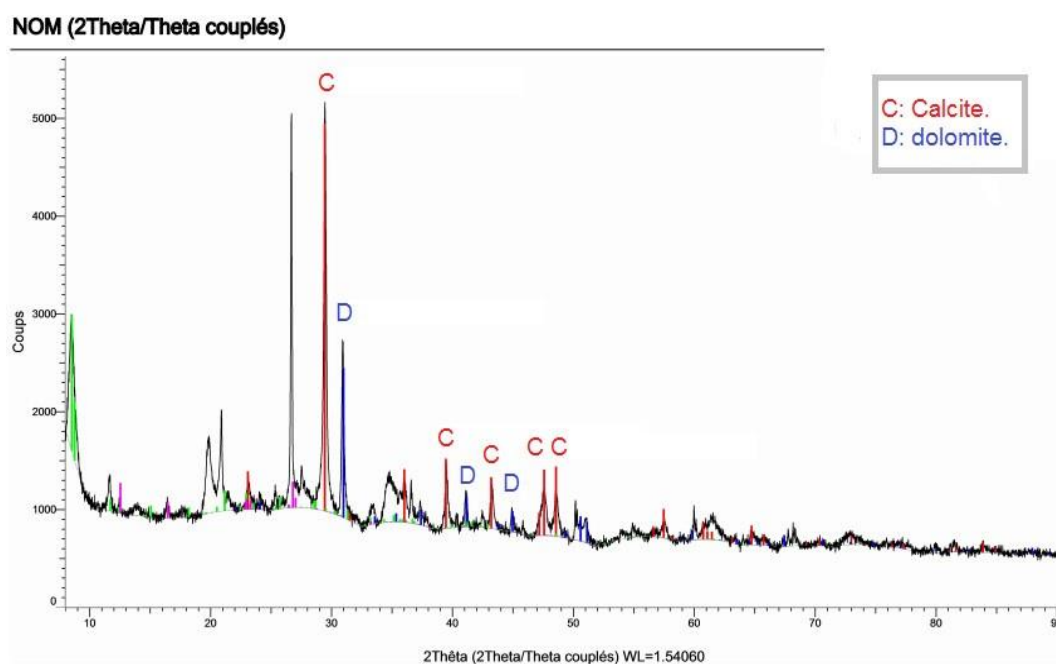


**Figure 4:** Histogram of the mineralogical DRX analyses of the red clay.

#### Chemical composition analysis by X-ray fluorescence

Clay's mineralogical and physico-chemical properties are particularly interesting in many applications such as water treatment, paint, barrier for pollutants, adsorbent, catalyst, etc. [25-48]. Table 2 lists the results of elemental chemical analysis obtained for the red and green claysamples. We can note that silica and aluminumconstitute the clay structure. The percentage of these compositions is very important. This resultindicates the presence of Kaolinite ( $Al_2Si_2O_5(OH)_4$ ).

Clay materials contain a relatively abundant amount of  $SiO_2$ . The ratio alumina/silica gives an idea of the permeability to water and moisture. The higher the ratio, the greater the permeability [49]. The results indicate

that the SiO<sub>2</sub>/Al<sub>2</sub>O<sub>3</sub> ratio equals 2.65 for the yellow clay, 3.28 for the green clay, and 3.72 for the red clay, indicating significant free silica content. The overall composition of other oxides (Fe<sub>2</sub>O<sub>3</sub>, MgO, K<sub>2</sub>O, and Na<sub>2</sub>O) reaches a percentage of 13.13%, 11.73%, and 20.85 % in the three types of clay (yellow, green, and red), which shows that our clay is not pure [50].

The yellow and red clay samples present a rather high K<sub>2</sub>O content (3.78% and 2.86%) compared to the green clay sample indicating that the yellow and the red clays are richer in illite, which confirms the results obtained by DRX. The high CaO content in the red clay indicates a high amount of calcium carbonate in this type of clay. The red clay sample contains a notable amount of calcium oxide CaO (31.71%). This result is quite consistent with the presence of a calcite phase detected by XRD.

**Table 2.** Chemical composition of the clay samples (yellow, green, and red).

Clay	SiO <sub>2</sub>	Al <sub>2</sub> O <sub>3</sub>	Fe <sub>2</sub> O <sub>3</sub>	CaO	MgO	SO <sub>3</sub>	K <sub>2</sub> O	Na <sub>2</sub> O
Yellow	36.66	13.82	5.44	15.63	3.71	0.85	3.78	0.20
Green	48.86	14.89	6.34	8.43	2.66	1.02	1.98	0.75
Red	38.41	10.31	10.53	31.71	7.41	3.21	2.86	0.05

### Infrared(IR) analysis

Infrared spectroscopy was used to complete the analysis of the clay sample. Figures 5, 6, and 7 illustrate the spectra obtained. Figure 5 presents the spectrum of the yellow clay. It can be observed that the peaks which spread between 3200-3800 cm<sup>-1</sup>, located at 3620.1 cm<sup>-1</sup> and 3417.6 cm<sup>-1</sup> correspond to the elongation vibrations of the internal OH groups. The peak ranges between 1600-1700 cm<sup>-1</sup> can be attributed to the valence vibrations of the OH group of the water of constitution and the bending vibrations of the adsorbed water's bending vibrations at 1649.0 cm<sup>-1</sup>. The peaks located between 1400 and 1500 cm<sup>-1</sup> are attributed to the deformation vibrations of the CH<sub>3</sub> groups located at 1442.6 cm<sup>-1</sup> [51,52]. The 877.6 cm<sup>-1</sup> peak corresponds to the presence of calcium carbonate CaCO<sub>3</sub> [53].

Figure 6 presents the spectrum of the green clay: The peaks that range between 3397.3 cm<sup>-1</sup>, 3421.5 cm<sup>-1</sup> and 3620.1 cm<sup>-1</sup> correspond to the elongation vibrations of the internal OH groups. The peak between 1770-1800 cm<sup>-1</sup> located at 1797.5 cm<sup>-1</sup> can be attributed to the elongation vibrations of the C=O [54]. The 871.8 cm<sup>-1</sup> peak corresponds to the presence of calcium carbonate CaCO<sub>3</sub>. The absorption peak at 779.2 cm<sup>-1</sup> is in agreement with the XRD, indicating the presence of quartz in the clay. Figure 7 shows the spectrum of the red clay: The peaks that range between 3633.6 cm<sup>-1</sup> and 3442.7 cm<sup>-1</sup> correspond to the elongation vibrations of the internal OH groups. The peak that ranges between 1600-1700 cm<sup>-1</sup> can be attributed to the valence vibrations of the OH group of the constituent water, in addition to the bending vibrations of the adsorbed water located at 1645.2 cm<sup>-1</sup>. The peaks located between 900-1200 cm<sup>-1</sup> correspond to the valence vibrations of the Si-O bond [55]. The 844.8 cm<sup>-1</sup> peak corresponds to the presence of calcium carbonate CaCO<sub>3</sub> [54].

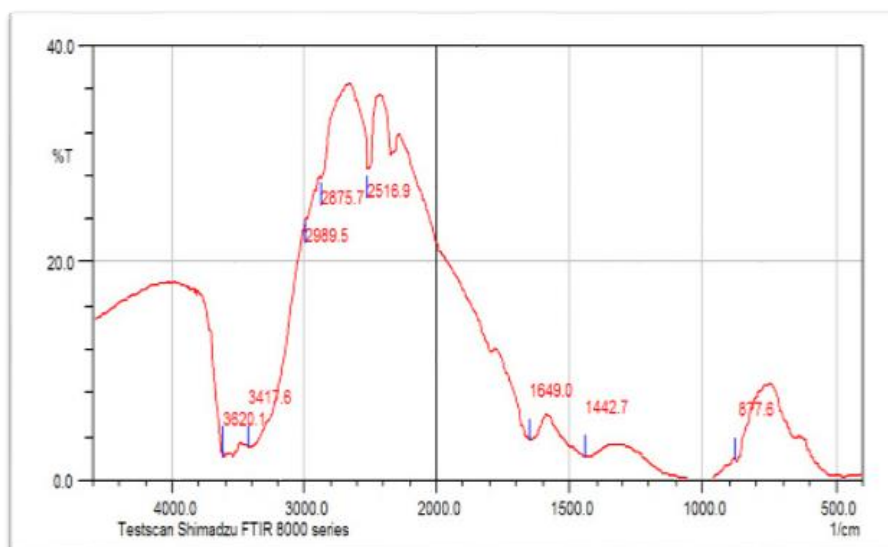


Figure 5. Infrared spectrum of yellow clay sample.

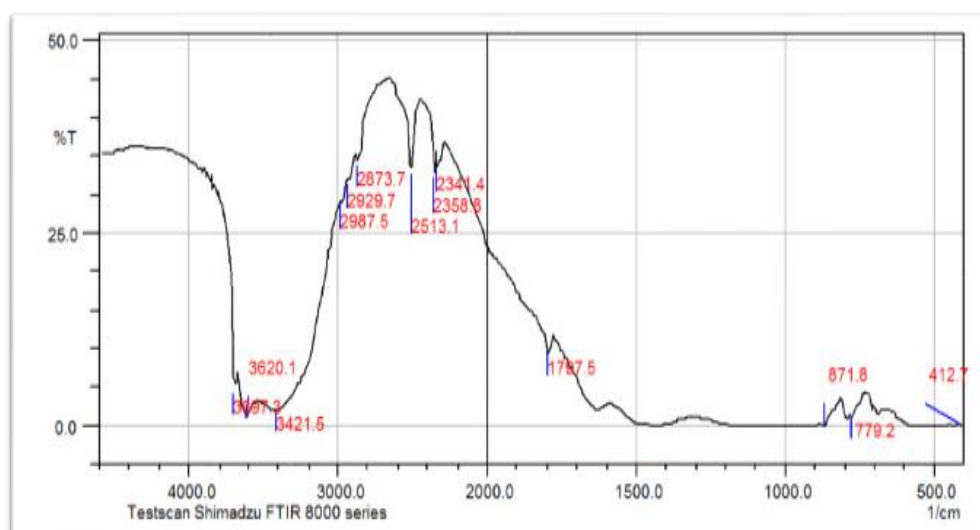
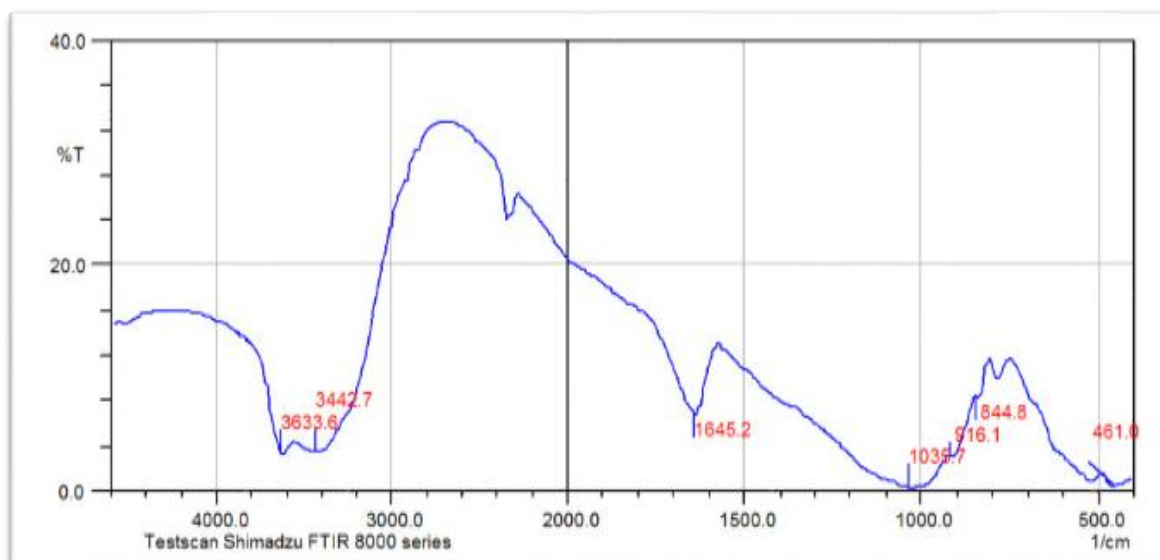


Figure 6. Infrared spectrum of green clay sample.



**Figure 7.** Infrared spectrum of red clay sample.

**Physico-chemical characterization of clay samples**

Table 3 gathers the values of the various parameters relating to our clay samples. We notice that the pH values obtained from the three clays (yellow, green, and red) are 9.18, 8.19, and 7.94, respectively. These results indicate the basicity of the studied samples, which would be due to the soluble salts and basic character as the alkaline carbonates and bicarbonates or the silicates, which generally return in the composition of the clay [56]. We note that the moisture content value is low for both yellow and green clay samples compared to the red clay sample. This explains the non-hygroscopic character and confirms the low value of porosity, which indicates that both yellow and green clay samples can be considered very low porous.

The value of colloidalilty for the three samples (yellow, green, and red) is low (1.9, 8.65, 9.44), which explains the low ionization of particles entering the constitution of the samples studied [57]. The loss on ignition corresponds to the loss of mass of a powder brought to the oven at 1000°C. In our case, we find a high value of about 17.52 % for the yellow clay, 19.96 % for the green clay, and 22.13 % for the red clay sample. The latter may be related to the presence of carbonate and silicate minerals [59]. The swelling coefficient of the studied samples of yellow clay, green clay, and red clay is 58.57 %, 54.08 %, and 55.39 %. According to the classification proposed by Holtz et al. [59], the studied samples can be considered as having a medium swelling coefficient.

**Table 3.** Physicochemical parameters of the clay sample.

Parameter	Yellow	Green	Red
pH	9.18	8.19	7.94
Moisture content H (%)	7.23	3.77	3.96
D	2.25	2.38	2.63
Swelling index I <sub>g</sub> (%)	58.57	54.08	55.39
Colloidalilty C (%)	1.9	8.65	9.44
Loss on fire PAF (%)	17.52	16.96	22.13

**The Atterberg limits**

Using Atterberg limits on our clay samples, it can be noted that the plasticity  $W_p$  values of the clay samples (yellow, green and red, respectively) reached 29.33 %, 38 %, and 34.33 % (Table 4). Figures 8, 9, and 10 indicate the values of clay liquidity  $W$  in the three samples: 34%, 50%, and 38.3 %. The plasticity index values  $I_p$  of the clay samples is 4.67 %, 12 %, and 3.97 %, respectively. According to the Atterberg limits classification presented in Table 5, it can be concluded that the two clays (yellow and red) have low plasticity and that the green clay has medium plasticity [59]. Bell [60] reported that the plasticity increases in the presence of quartz, kaolinite, and decreases for montmorillonite. Dash and Hussain [61] reported the same result. The authors explained that plasticity would be increased in silica-rich soils ( $Si^{2+}$  is the main ion in quartz and kaolinite). In the case of green clay, a significant percentage of quartz (27.04 %) is obtained with the help of the DRX analysis. Thus, the plasticity index has a maximum value (12 %).

**Table 4.** Values of the Atterberg limits.

Clay	Liquidity limit $W_L$ (%)	Plasticity limit $W_p$ (%)	Plasticity Index $I_p$ (%)
Yellow	34	29.33	4.67
Green	50	38	12
Red	38.3	34.33	3.97

**Table 5.** Classification of clay based on the Atterberg limits [24].

Plasticity index $I_p$ (%)	< 7	from 7 to 17	> 7
Plasticity	Low	Average	High

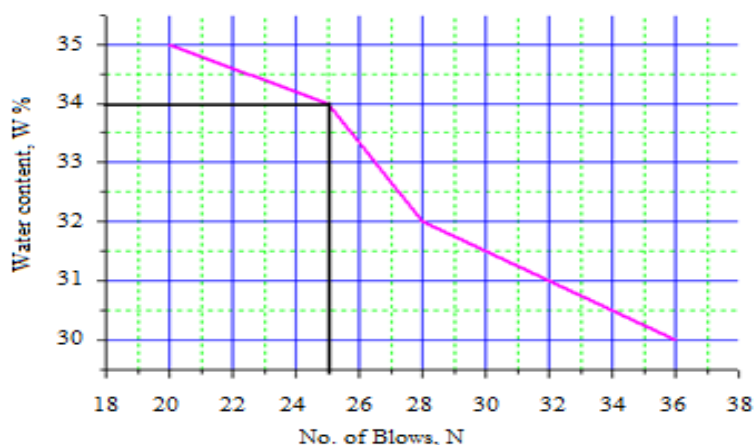


**Figure 8.** Diagram for the determination of the liquidity limit of yellow clay.

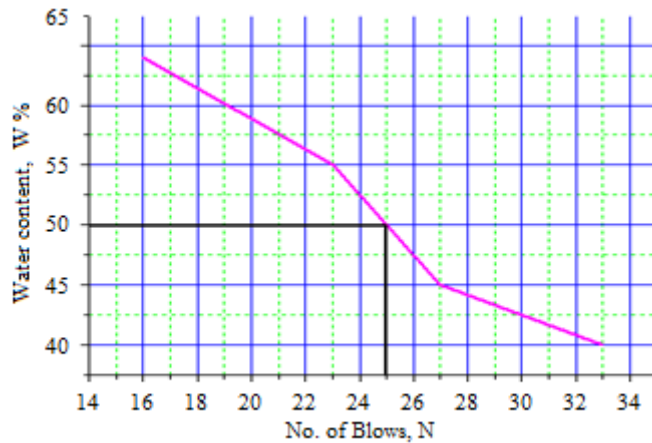


**Figure 9.** Diagram for the determination of the liquidity limit of green clay

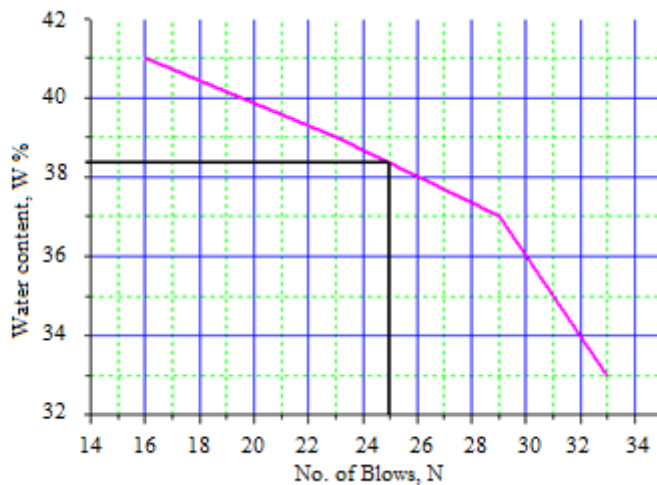


**Figure 10.** Diagram for the determination of the liquidity limit of red clay.

#### IV. Conclusion

This paper highlighted the importance of clay, a very abundant material in Algeria, for rural construction when used properly. The experimental techniques allowed us to highlight the phyllite and mineral phases and the chemical composition of the clays analyzed. The results indicate that the three types of clay of Mâadid of the region of M'sila constitute kaolinite, illite, and calcite as associated clay minerals. These findings also highlighted the richness of these three types of clay (yellow clay, green clay, and red clay) in quartz, translating into a high proportion of silica and low porosity. According to the results obtained, it can be said that the red clay sample is the most profitable and close to being used in the manufacture of cement with processing recommendations such as using limestone from a quarry with low  $SO_3$  as a mixture to ensure the conformity of cement quality. Therefore, it is important to consider the results obtained before applying this type of clay to prepare composite materials for rural construction.

#### References

[1] Modélisation multi-échelles des propriétés élastiques du composite argile-pailles de riz. Thèse doctorat. Christian Enagnon ADADJA ; 16 Juillet 2020 . Université d'Abomey-Calavi et Université de Lorraine.

[2] Safa Tahmasebi, Mohamed A El-Esawi, Zaid Hameed Mahmoud, Anton Timoshin, Hamed Valizadeh, Leila Roshangar, Mojtaba Varshoch, Aydin Vaez, Saeed Aslani, Jamshid G Navashenaq, Leili Aghebati-Maleki, Majid Ahmadi. Immunomodulatory effects of Nanocurcumin on Th17 cell responses in mild and severe COVID-19 patients, *Journal of cellular physiology*, 236(7):5325, 2021.

[3] Zaid H.M. The magnetic properties of alpha phase for iron oxide NPs that prepared from its salt by novel photolysis method, *Journal of Chemical and Pharmaceutical Research*. 9(8);29-33, 2017.

[4] M Kavitha, Zaid Hamid Mahmoud, Kakarla Hari Kishore, AM Petrov, Aleksandr Lekomtsev, Pavel Iliushin, Angelina Olegovna Zekiy, Mohammad Salmani. Application of Steinberg model for vibration lifetime evaluation of SN-AG-CU-based solder joints in power semiconductors, *IEEE Transactions on Components, Packaging and Manufacturing Technology*. 11(3) :444-450, 2021.

[5] C.D. Atis, O. Karahan, Properties of steel fiber reinforced fly ash concrete. *Construction and building Materials* 23(2009)392-399.

[6] Hussein Kadhim Sharaf, Sadeq Salman, Marwah H Abdulateef, Rustem R Magizov, Vasili Ivanovich Troitskii, Zaid Hameed Mahmoud, Rafis H Mukhutdinov, Harsha Mohanty. Role of initial stored energy on hydrogen microalloying of ZrCoAl (Nb) bulk metallic glasses, *Applied Physics A.*, 127(1) :1-7, 2021.

[7] Zaid Hamid Mahmoud, Hanif Barazandeh, Seyed Mojtaba Mostafavi, Kirill Ershov, Andrey Goncharov, Alexey S Kuznetsov, Olga D Kravchenko, Yu Zhu. Identification of rejuvenation and relaxation regions in a Zr-based metallic glass induced by laser shock peening, *Journal of Materials Research and Technology*. 11 :2015-2020.

[8] Zaid Hamid Mahmoud, Marwa Sabbar Falih, Omaira Emad Khalaf, Mohammed Alwan Farhan, Farah Kefah Ali. Photosynthesis of AgBr Doping TiO<sub>2</sub> Nanoparticles and degradation of reactive red 120 dye. *Journal of Advanced Pharmacy Education & Research*, 8(4), 2018.

[9] Abakar Ali, Caractéristiques mécaniques et thermiques de l'argile stabilisée par la gomme arabique et renforcée par la paille de riz, Thèse doctorat, Université de Lorraine, 2018

[10] HM Zaid, Synthesis of Bismuth oxide Nano powders via electrolysis method and study the effect of change voltage on the size for it. *Australian journal of basic and applied sciences*. 11(7) :97-101.

[11] Zaid H.M. Effect of Au doping on the magnetic properties of Fe<sub>3</sub>O<sub>4</sub> NPs prepared via photolysis and co-precipitation methods. *Diyala journal for pure sciences*. 14(3), 2018.

[12] Zaid Hamid Mahmoud, Nuha Farhan Abdul Kareem, Aklas Ahmed Abdul Kareem. Effect of solvents on size of copper oxide nanoparticles fabricated using photolysis method. *Asian Journal of chemistry*, 30(1) :223-225, 2018.

[13] Rawnaq B Jimaa, Zaid H Mahmoud, Farah K Ali. Evaluation the efficiency of  $\text{CuFe}_2\text{O}_4$  prepared photolysis by OSD and photo degradation. *Entomol. Appl. Sci. Lett.*, 5(2) :91-100, 2018.

[14] Indah Raya, Hamzah H Kzar, Zaid Hameed Mahmoud, Alim Al Ayub Ahmed, Aygul Z Ibatova, Ehsan Kianfar. A review of gas sensors based on carbon nanomaterial. *Carbon Letters.*, 32, 339-364, (2022).

[15] Z.Koadri, A. Benyahia, N. Deghfel, K. Belmokre, B. Nouibat, A. Redjem. Étude de l'effet du temps de traitement alcalin de fibres palmier sur le comportement mécanique des matériaux à base d'argile rouge de la région de M'sila, *Matériaux & Techniques* 107, 404 (2019) pp.1-11 <https://doi.org/10.1051/mattech/2019031>

[16] F. Mouissa, A. Benyahia, M. Djehiche, K. Belmokre, N. Deghfel, A. Redjem, and Z. E. A. Rahmouni. The effect of chemical treatment on the mechanical and thermal properties of composite materials based on clay reinforced with sawdust. *Matériaux & Techniques* 109, 101 (2021) pp.1-10 <https://doi.org/10.1051/mattech/2021013>

[17] Tuan Anh PHUNG, Malo LE GUERN, Mohamed BOUTOUIL, Valorisation des terres et argiles en bâtiment : performances mécaniques, Conférence Internationale Francophone No MaD 2015 Mines Douai, France 5-6 Novembre 2015.

[18] Amin N.C., Andji Y.Y.J., Ake M., Yolou S.F., Toure Abba A., Kra Gabrielle J., *J. Sci. Pharm. Biol.* 10 (2009) 21.

[19] Zaid Hamid Mahmoud, Rasoul Fakhrie Khudeer. Spectroscopy and structural study of oxidative degradation Congo Red Dye under sunlight using  $\text{TiO}_2/\text{Cr}_2\text{O}_3\text{-CdS}$  nanocomposite. *International Journal of ChemTech Research*, 12(3) :64-71, 2019.

[20] Mohammed Alwan Farhan, Zaid Hamid Mahmoud, Marwa Sabbar Falih. Synthesis and characterization of  $\text{TiO}_2/\text{Au}$  nanocomposite using UV-Irradiation method and its photocatalytic activity to degradation of methylene blue. *Asian J. Chem.*, 30(5) :1142-1146, 2018.

[21] Wijdan Amer Ibrahim, Zaid Hamid Mahmoud. Synthesis and characterization of new Fe-complex and its nanoparticle oxide using the novel photolysis method. *International Journal of Pharmaceutical and Phytopharmacological Research.*, 8 :51-61, 2018.

[22] Chossat J.C., *La mesure de la conductivité hydraulique dans les sols – Choix des méthodes*, 2005, Lavoisier, USA: 720 pp.

[23] Rollet P., Bouaziz R., *L'analyse thermique- les changements de phase*. ED. Gautier-Villard, Tome1, Paris, (1972).

[24] Gillot, E. Jack, *Clay engineering geology*. John Wiley et Sons, Inc. (1984).

[25] Qlihaa, A., Dhimni, S., Melrhaka, F., Hajjaji, N., & Srhiri, A. (2016). Caractérisation physico-chimique d'une argile Marocaine [Physico-chemical characterization of a Moroccan clay]. *Journal of Materials and Environmental Science*, 7(5), 1741-1750.

[26] Hamid Zaid, Ahmed Najem. Synthesis of  $\alpha$ -Fe<sub>2</sub>O<sub>3</sub> Nano Powders by Novel UV Irradiation Method. *diyala journal for pure sciences*, 14(1) :56, 2018.

[27] Zaid Hamid Mahmoud, Akla Ahmed Abdalkareem. Removal of Pb ions from Water by Magnetic Iron Oxide Nanoparticles that Prepared via ECD. *European Journal of Scientific Research* 145(4) (2017), 354-365.

[28] Brunet F. (1986) Thèse de Docteur en Pharmacie de l'Université de Paris XI, France.

[29] Noor Sabah Al-Obaidi, Zaid Hamid Mahmoud, Ahlam Ahmed Frayyih Anfal S Ali, Farah K Ali. Evaluating the electric properties of poly aniline with doping ZnO and  $\alpha$ -Fe<sub>2</sub>O<sub>3</sub> nanoparticles. *Pharmacophore*, 9(5) :61-67, 2018.

[30] Zaid Hamid Mahmoud, Karim H Hassan, Omar Dheyaa Abdul Sattar, Kefah Ali Farah. Low Temperature Novel Photosynthesis Method and Characterization of ZnO/CuO Nano composite., *Journal of Biochemical Technology*, 9(3) :1, 2018

[31] Ashkan Bahadoran, Mahmoud Khoshnoudi Jabarabadi, Zaid Hameed Mahmood, Dmitry Bokov, Baadal Jushi Janani, Ali Fakhri. Quick and sensitive colorimetric detection of amino acid with functionalized-silver/copper nanoparticles in the presence of cross linker, and bacteria detection by using DNA-template nanoparticles as peroxidase activity. *Spectrochimica Acta Part A: Molecular and Biomolecular Spectroscopy*, 268 :120636, 2022.

[32] Prasad M.S., Reid K.J. & Kaolin: processing, properties and applications. *Applied Clay Science*, 6(2), 87-119. Murray H.H. (1991)

[33] Zaid Mahmoud, Omaima Emad Khalaf, Mohammed Alwan Farhan. Novel photosynthesis of CeO<sub>2</sub> nanoparticles from its salt with structural and spectral study. *Egyptian Journal of Chemistry*, 62(1):141-148, 2019.

[34] Zaid Hamid Mahmoud, Marwah Hashim, Farah Kefah Ali. Low temperature photosynthesis of Bi<sub>2</sub>O<sub>3</sub> nano powder. *Earthline Journal of Chemical Sciences*, 2(2):301-307, 2019.

[35] Nuha Abdul Jaleel Omran, Zaid Hamid Mahmoud, Noor Kadhum Ahmed, Kefah Ali Farah. Low-temperature synthesis of  $\alpha$ -Fe<sub>2</sub>O<sub>3</sub>/MWCNTs as photo-catalyst for degradation of organic pollutants. *Oriental Journal of Chemistry*, 35(1):332, 2019.

[36] Konta J. (1995) Clay and man: Clay raw materials in the service of man. *Applied Clay Science*, 10, 275-335.

[37]Zaid H Mahmoud, Reem Adham AL-Bayati, Anees A Khadom. Synthesis and supercapacitor performance of polyaniline-titanium dioxide-samarium oxide (PANI/TiO<sub>2</sub>-Sm<sub>2</sub>O<sub>3</sub>) nanocomposite. Chemical Papers., 76(3):1401-1412, 2022.

[38]Zaid Hameed Mahmoud, Omar Dhaa Abdalstar, Noor Sabah. Semiconductor metal oxide nanoparticles: a review for the potential of H<sub>2</sub>S gas sensor application. Earthline Journal of Chemical Sciences., 4(2):199-208, 2020.

[39]Zaid H Mahmoud, Reem Adham AL-Bayati, Anees A Khadom. Modified anatase phase of TiO<sub>2</sub> by WO<sub>3</sub> nanoparticles: Structural, morphology and spectral evaluations. Materials Today: Proceedings, 2021.

[40] Harvey C.C. & Murray H.H. (1997) Industrial clays in the 21<sup>st</sup> century: A perspective of exploration, technology and utilization. Applied Clay Science, **11**, 285-310.

[41]Siswanto, W.A., Borodin, K., Mahmoud, Z.H., Surendar, A., Sajjadifar, S., Abdilova, G. and Chang, J. (2021), "Role of aging temperature on thermomechanical fatigue lifetime of solder joints in electronic systems", Soldering & Surface Mount Technology, Vol. 33 No. 4, pp. 232-239. <https://doi.org/10.1108/SSMT-07-2020-0029>.

[42] Zaid H Mahmoud, Reem Adham AL-Bayati, Anees A Khadom. The efficacy of samarium loaded titanium dioxide (Sm: TiO<sub>2</sub>) for enhanced photocatalytic removal of rhodamine B dye in natural sunlight exposure. Journal of Molecular Structure., 1253, 132267, 2022.

[43]Asep Suryatna, Indah Raya, Lakshmi Thangavelu, Firas Rahi Alhachami, Mustafa M Kadhim, Usama S Altamari, Zaid H Mahmoud, Yasser Fakri Mustafa, Ehsan Kianfar. A Review of High-Energy Density Lithium-Air Battery Technology: Investigating the Effect of Oxides and Nanocatalysts. Journal of Chemistry., 2022, 2022.

[44] Ekosse G.E. (2000) The Mokoro kaolin deposit, south eastern Botswana: Its genesis and possible industrial applications. Applied Clay Science, **16**, 301-320.

[45]Jasim, S.A., Ali, M.H., Mahmood, Z.H. et al. Role of Alloying Composition on Mechanical Properties of CuZr Metallic Glasses During the Nanoindentation Process. Met. Mater. Int. (2022). <https://doi.org/10.1007/s12540-021-01164-7>.

[46]Raya, I., Widjaja, G., Mahmood, Z.H. et al. Kinetic, isotherm, and thermodynamic studies on Cr(VI) adsorption using cellulose acetate/graphene oxide composite nanofibers. Appl. Phys. A 128, 167 (2022). <https://doi.org/10.1007/s00339-022-05307-4>.

[47]Mahmoud, Z.H., AL-Bayati, R.A. & Khadom, A.A. Electron transport in dye-sanitized solar cell with tin-doped titanium dioxide as photoanode materials. J Mater Sci: Mater Electron 33, 5009–5023 (2022). <https://doi.org/10.1007/s10854-021-07690-9>.

[48] Carretero M.I. (2002) Clays minerals and their beneficial effects upon human health. Applied Clay Science, **21**(21), 155-163.

- [49] Sadki H., Ziat K. et Saidi M., J. Mater. Environ. Sci. 5 (S1) (2014) 2061.
- [50] W.G. Holtz, Gibbs « Engineering properties of expansive clays» Transactions, ASCE 121, 641 (1956).
- [51] M. Gourouza, A. Zanguina, I. Natatou, A. Boos, Rev. CAMES \_ Sciences Struct. Mat. 1, 29 (2013).
- [52] O. Qabaqous, N. Tijani, M. Naciri Bennani, A. El Krouk, J. Mater. Environ. Sci. 5, 2247 (2014).
- [53] A. Lahsini, J. Bentama, A. Addaou, M. Rafiq, J. Chim. Phys. 95, 1001 (1998)
- [54] A. Lahsini, J. Bentama, A. Addaou, M. Rafiq, Caractérisation physico-chimique et étude de frittage d'une argile destinée à l'élaboration de membranes de filtration tangentielle, J. Chim. Phys. 95 (1998) 1001-1019 20
- [55] A. Arfane, A. Salhi, M. El Krati, S. Tahiri, M. Monkade, E.K. Lhadi., M. Bensitel, Etude cinétique et thermodynamique de l'adsorption des colorants Red 195 et Bleu de méthylène en milieu aqueux sur cendres volantes et les mâchefers, J. Mater. Environ. Sci. 5(6) (2014) 1927-1939
- [56] Edahbi M., M. Khaddor, F. Salmoun, J. Mater. Environ. Sci. 5 (S1) (2014) 2135.
- [57] Rollet P., Bouaziz R., L'analyse thermique- les changements de phase. ED. Gautier-Villard, Tome1, Paris, (1972).
- [58] W.G. Holtz, Gibbs «Engineering properties of expansive clays» Transactions, ASCE 121, 641 (1956).
- [59] Norme française NFP 94–051 Détermination des limites d'Atterberg: limite de liquidité à la coupelle, limite de plasticité au rouleau, 16 p(1993).
- [60] Bell, F. [1996], 'Lime stabilization of clay minerals and soils', Engineering geology 42(4), 223-237.
- [61] Dash, S. K. and Hussain, M. [2011], 'Lime stabilization of soils : Reappraisal', Journal of Materials in Civil Engineering 24(6), 707 - 714.